

Inelastic neutron scattering study of methyl tunnelling in an oriented single-crystal of 2,6-dimethylpyrazine at low temperature and rotational–potential calculations

B. Nicolai^{a,*}, E. Kaiser^b, F. Fillaux^c, G.J. Kearley^a, A. Cousson^b, W. Paulus^{b,d}

^a Institut Laue-Langevin BP 156, 38042 Grenoble Cedex 09, France

^b Laboratoire Leon Brillouin, CEA de Saclay, 91161 Gif sur Yvette Cedex, France

^c LASIR-CNRS, 2 Rue Henry-Dunant, 94320 Thiais, France

^d Institute für Crystallographie, RWTH Aachen, Järgenstrasse, 17-19 D-52059 Aachen, Germany

Received 7 May 1997; in final form 1 September 1997

Abstract

Inelastic neutron scattering (INS) on an oriented single-crystal is used to assign directly the tunnelling splittings to the two crystallographically-inequivalent methyl groups in 2,6-dimethylpyrazine ($C_6N_2H_8$) at 2 K. Their antiparallel conformation found by crystallography and their respective rotational barriers are reproduced by a combination of ab-initio and molecular mechanics calculations. These results are used for a better understanding of the methyl groups dynamics. © 1998 Elsevier Science B.V.

1. Introduction

Rotational-tunnelling frequencies are very sensitive probes for the local rotational potential experienced by rotors such as methyl groups in molecular crystals [1]. The aim of this paper is to correlate the observed potentials with the structural data and extract dynamical information [2]. CH_3 side groups attached to aromatic rings have been extensively studied for tunnelling (for example, derivatives of the benzene: Toluene [3], *p*-xylene [4,5], halogenomesithylenes [6,7], and derivatives of pyridine: γ -picoline [8] and lutidine [9]). In the gas phase, these methyl groups are almost free rotors

and, in the crystalline state, they have low rotational barriers and a large tunnel splitting which is observable by INS.

The low-temperature structure of 2,6-dimethylpyrazine has recently been solved and contains two crystallographically inequivalent methyl groups attached to the aromatic pyrazine ring [10]. Each of the methyl groups experiences a different potential due to environmental differences. The INS spectrum exhibits two tunnelling lines at 20 and 29 μ eV and two libration lines at 8 and 10 meV, each one due to a crystallographically-distinct methyl group. Assignment can be directly made by inspection of the tunnelling–excitation intensity as a function of the momentum-transfer direction in an oriented single-crystal. Moreover, in the crystal at low temperature, the two methyl groups are in a fixed conformation.

* Corresponding author. Tel.: +33-76207232; fax: +33-76483906; e-mail: nicolai@ill.fr.

We have investigated their specific dynamics by calculation of the rotational potential from the crystal structure, using GAMESS-UK ab-initio program [11] and Cerius² molecular mechanics software [12].

2. Prerequisites

2.1. Crystal structure

The calculation of the rotational potential is based on exact structural information. They will be compared to experimental rotational parameters. The crystalline structure, unknown up to now, was determined by a preliminary X-ray diffraction at 253 K [13]. Neutron-diffraction structure-determination on an hydrogenated single-crystal of 2,6-dimethylpyrazine, at sample temperatures of 260, 20 and 5 K confirmed the space group. The lattice parameters and accurate positions for protons were followed in function of the temperature. Significant differences were found between the lattice parameters at temperatures of 260 K and lower, but the conformation of the molecule was similar at all temperatures. [10].

The space group is P 1 21/a 1 (monoclinic) with four formula-units per unit cell. The structure consists of parallel layers of planar molecules perpendicular to the $(-2\ 0\ 1)$ plane. The lattice parameters are at 5 K, $a = 7.2875(132)$, $b = 10.7247(185)$, $c = 7.4517(118)$ Å, $\beta = 90.369(138)^\circ$. The details of the

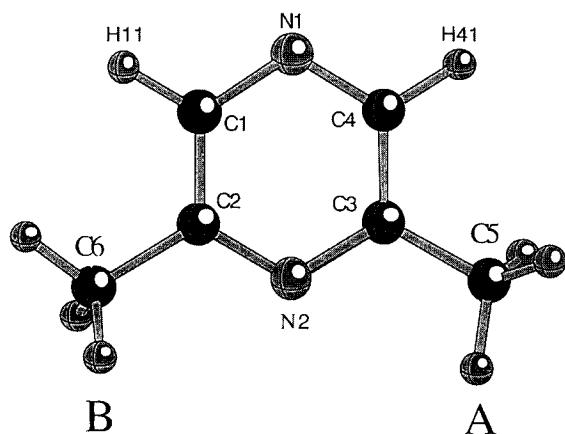


Fig. 1. AB conformation of the 2 methyl groups C5- and C6-types in the crystalline state.

structure determination will be published elsewhere [10].

There are clearly two different environments for the methyl groups C5 and C6 linked to the same pyrazine ring (Fig. 1). Therefore, they experience two different local potentials. For the two groups, there is a proton almost in the molecular plane but the orientation of these protons are found to be the same: C5-type presents a C–H bond almost in the molecular plane oriented through the N atom, C6-type is obtained by rotation of $61(\pm 10)^\circ$.

2.2. The rotational potential

According to quantum mechanics, the energy of a molecule can be obtained by solution of the Schrödinger equation. The case of a hindered symmetric rigid rotor (one dimensional), with a fixed rotational axis, can be solved using the single-particle approach [1]:

$$\left(-\frac{\hbar^2}{2I_r} \frac{\partial^2}{\partial \phi^2} + V(\phi) \right) \psi = E\psi \quad (1)$$

where I_r is the reduced moment of inertia of the rotor and ϕ is the angular coordinate $-\frac{\hbar^2}{2I_r} \frac{\partial^2}{\partial \phi^2}$ is the kinetic operator (the Hamiltonian for a free rotor), $V(\phi)$ is the local static crystalline rotational potential. Because the methyl group has a threefold symmetry, $V(\phi)$ is periodic and can be expanded in Fourier series:

$$V(\phi) = \sum_n \frac{1}{2} V_{3n} (1 - \cos[3n\phi + \delta_{3n}]) \quad (2)$$

V_{3n} is the amplitude of the 3 n -fold contribution and δ_{3n} is a phase. According to the threefold symmetry, there are two types of rotor wave-functions A and E , E being doubly degenerate. The energy levels are calculated by diagonalization of the Hamiltonian. There are two kinds of excitations: Librational and tunnelling transitions. The librational transitions describe the oscillations of the molecule in one minimum of the potential, each librational state is split into two tunnelling states owing to the overlap of the wave-functions in the adjacent wells of the potential.

The observed tunnel-splitting ν_t is related to the strength and the shape of the rotational potential. The exponential variation of ν_t as a function of the

rotational potential makes tunnelling spectroscopy a very sensitive probe of the molecular crystal-potentials, and there is a strong dependence of the tunnel splitting and the individual components of these crystalline potentials. This is the simplest approach to methyl rotation, other theoretical models have been developed: pair of coupled rotors [14–16], coupling with phonons [17], infinite chain of coupled methyl groups [18–20] and coupling with centre of mass translation [21–23].

We evaluated the rotational potential in 2 parts: The internal contribution by an ab-initio method and the external by molecular mechanics (or empirical force-field calculations).

3. Experimental

The neutron-scattering experiments were carried out on an oriented hydrogenated single-crystal sample at 1.7 K using the IN10B backscattering spectrometer at the Institut Laue-Langevin (Grenoble, France). The incident energy was changed using thermal expansion of the monochromator KCl (200). The crystal analysers (unpolished Si(111)) backscatter neutrons with 6.27 Å wavelength. The monochromator and the analysers provide a resolution of 1 μeV and a momentum transfer range from 0.3 to 1.8 \AA^{-1} .

The title compound is a commercial product. A large colourless single-crystal was grown using the Bridgman technique (5 cm height, 1 cm diameter) [13]. Due to its hygroscopic nature and its melting point of 311 K, the sample was handled under dry helium atmosphere at low temperature and loaded into a standard liquid helium cryostat.

We obtained the INS spectra in the methyl group librational region using powder sample on the time-of-flight IN5 spectrometer at the Institut Laue-Langevin. IN5 is a direct geometry spectrometer. It uses four disk-choppers to produce the mono-energetic neutron beam. We used an incident wavelength of 2 Å, the energy resolution being 1.71 meV to measure libration transitions. And we used an incident wavelength of 13 Å, the energy resolution being 5.9 μeV at different sample temperatures to measure temperature dependence of the tunnelling frequencies. The commercially available 2,6-dimethylpyrazine (Al-

drich) was used without further purification and manipulated under dry nitrogen atmosphere at low temperature.

4. Results

INS spectra provide unique information on proton dynamics: The intensity depends on the atomic displacements and cross-sections, and because the cross section of the hydrogen is almost ten times greater than for any other atom, we observe mainly transitions involving hydrogen atom displacement.

For the single-crystal experiment on IN10B, the momentum transfer was parallel to the molecular plane, but the orientation of the momentum transfer in the plane was not determined. We had to choose the first orientation as the origin of the coordinate system. We took a series of spectra, the single-crystal being rotated around an axis perpendicular to the molecular plane (–2 0 1). For a single-crystal of thickness 1 cm, multiple scattering effects cannot be neglected. Second (or higher) order scattering results from successive scattering processes with wave vector change. At small scattering angles, the spectra are dominated by multiple scattering. For larger values of the scattering angle, the intensity of the single

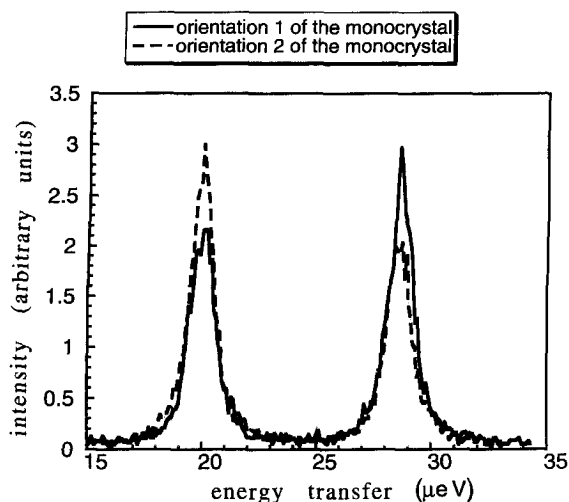


Fig. 2. Inelastic spectra of the single crystal of 2,6-dimethylpyrazine measured on IN10B at 1.7 K for 2 orientations of the single crystal.

inelastic-scattering event increases and can be greater than the multiple scattering contribution to the intensity. We did not correct the effect of multiple scattering and the tunnelling frequencies, the intensity results from single and multiple scattering, leading us only to qualitative analysis of the inelastic spectra. However, we observe 2 tunnelling lines located at 20 and 29 μeV . Such low-energy transitions can only be due to methyl tunnelling, one due of each of the 2 methyl groups. By rotating the single-crystal, the 2 tunnelling lines vary sinusoidally in intensity as a function of the orientation of the crystal and the intensity from each methyl group passes through a maximum twice per revolution as the H plane of the methyl groups coincides with the direction of momentum transfer vector, \vec{Q} (Fig. 2). All the equivalent C5-type methyl groups have their H-plane aligned along almost the same direction, whereas the C6-type H-plane are aligned along two very different directions at ca. $\pm 120^\circ$ from each other. The two observed tunnelling frequencies were assigned by comparison of the two maps $S(Q_x, Q_y, 29 \mu\text{eV})$ and $S(Q_x, Q_y, 20 \mu\text{eV})$. The intensity is represented as a function of the orientation of the momentum transfer Q (Fig. 3a and b, respectively). The first map shows only two maxima at ca. 0° – 180° , whilst the other one presents four maxima situated at ca. 60° and ca. 120° . We can now unambiguously assign the frequency of 20 μeV to the C6-type and of 29 μeV to the C5-type (Fig. 4).

The librational spectra recorded at 1.5 and 25 K are shown in Fig. 5. The strongest features in the spectrum are the two lines 8 and 10 meV. These 2 lines broaden on warming and merge together and are assigned to methyl liberations. This is in good agreement with a Raman band measured in a previous study on the solid compound at 8.4 meV (68 cm^{-1}) [24]. At lower energy transfer, the spectrum exhibits a very broad peak at about 4 meV, typical of a lattice phonon, this is again in good agreement with the Raman study which shows a lattice mode at 4.1 meV (33 cm^{-1}) [24]. At higher energy transfer, a broad line appears at 14 meV, which may also be attributed to lattice modes. If we consider pure three-fold potentials, the barrier heights, derived from the low-temperature tunnelling-lines, would be 24.4 and 21.7 meV, for the C6-type and the C5-type, respectively, assuming a rotational constant $B = 0.647$

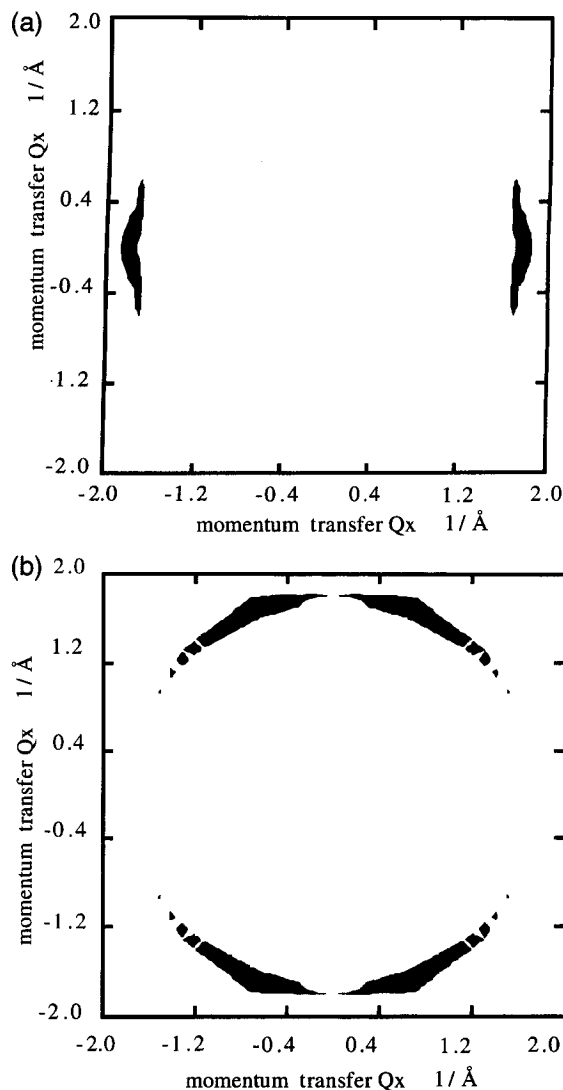


Fig. 3. Maps $S(Q_x, Q_y, \omega)$ represents the intensity of tunnelling peaks as a function of the momentum transfer. For clarity, only intensity around the maxima is illustrated. No useful information could be obtained for the intensity dependence on the modulus of Q due to limited counting statistics; (a) $\omega = 29 \mu\text{eV}$; (b) $\omega = 20 \mu\text{eV}$.

meV. The calculated librational energy is 10.05 and 9.3 meV for the C6-type and the C5-type, respectively, which corresponds quite well with the measurements. Because a single parameter, V_3 , repro-

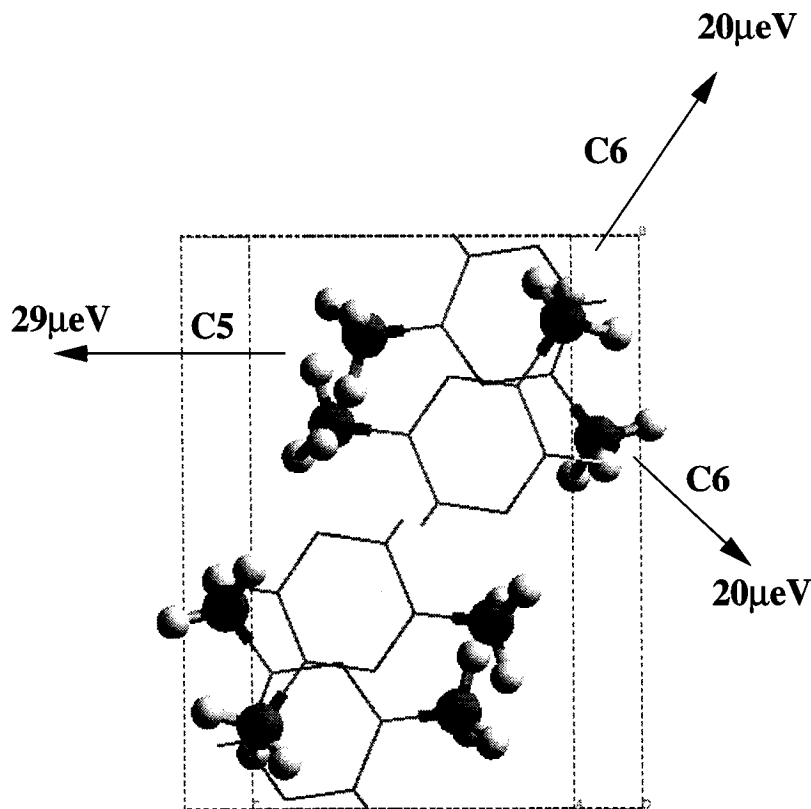


Fig. 4. Crystalline structure of 2,6-dimethylpyrazine at 5 K drawing assignment of the 2 tunnelling peaks 20 and 29 μeV to each of the C6-type and C5-type methyl groups.

duces both the tunnelling and librational transitions well, we conclude that higher terms are negligible.

The temperature dependence of the two tunnelling

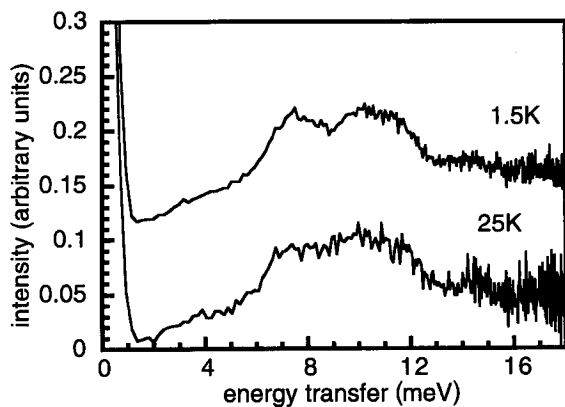


Fig. 5. The inelastic spectra in the methyl group librational region of 2,6-dimethylpyrazine measured on IN5 with an incident wavelength of 2 Å.

lines were measured in the temperature range from 1.5 to 30 K on IN5 (Fig. 6a). The two tunnelling lines are less well resolved than on IN10B. However, there is clearly a broadening and a shift towards lower frequencies for the two tunnelling lines, on warming. Such phenomena have been already observed in many compounds. Coupling with lattice displacements (phonons), which are increasingly populated with temperature, is responsible for the observed phenomena. The observed tunnelling frequency ν_{obs} being represented by the following equation: $\nu_{\text{obs}} = \nu_0 - \nu_1 \exp(-E_v/kT)$ (Fig. 6b). The peak broadening can be described by the following exponential expression: $w_{\text{obs}} = w_0 + w_1 \exp(-E_b/kT)$ (Fig. 6c). ν_0 represents the tunnelling frequency of the fundamental librational level, ν_1 of the first excited level, E_v and E_b the activation energies of the shift and the broadening, respectively, and k the Boltzmann constant. For each peak, the observed activation energies E_v and E_b are on

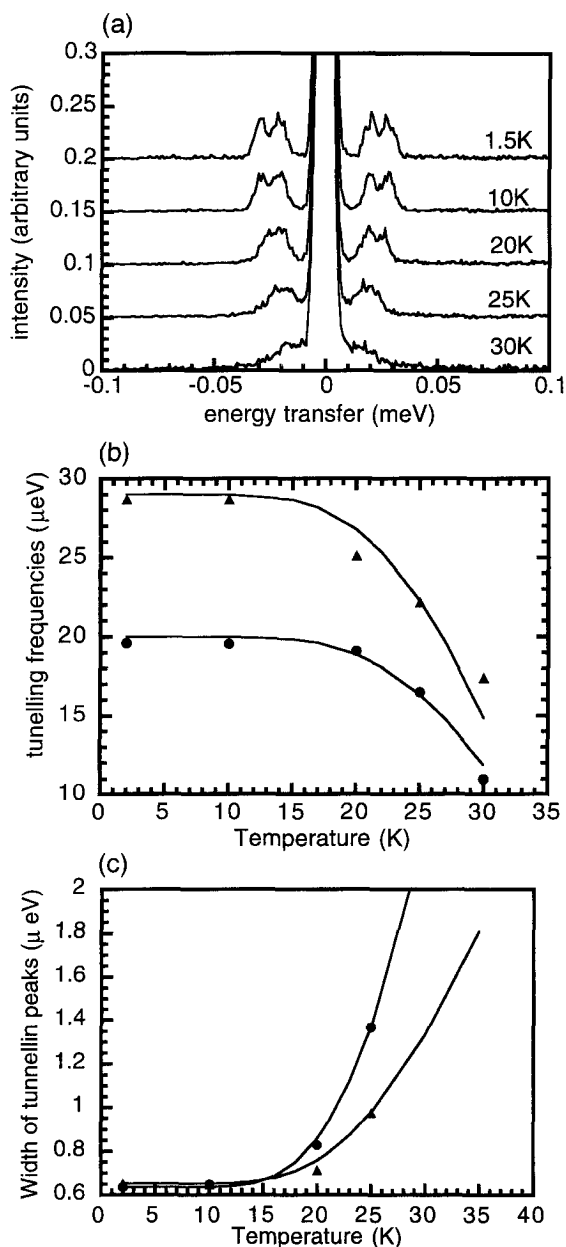


Fig. 6. (a) The temperature dependence of the tunnelling spectrum of 2,6-dimethylpyrazine measured on IN5 with an incident wavelength of 13 Å; (b) the tunnelling frequencies at 5 temperatures, the experimental values are represented by solid circles for the C6-type and solid triangles for the C5-type the curves being: $\nu_{\text{obs}} = 20 - 430 \exp(-10.3/kT)$ for the C6-type and $\nu_{\text{obs}} = 29 - 576 \exp(-9.59/kT)$ for the C5-type; (c) width of the tunnelling lines at 4 temperatures, the experimental values are represented by solid circles for the C6-type and solid triangles for the C5-type the curves being: $w_{\text{obs}} = 0.635 + 444.7 \exp(-10.3/kT)$ for the C6-type and $w_{\text{obs}} = 0.651 + 127.82 \exp(-9.59/kT)$ for the C5-type.

the same order of magnitude, E_b being close to the experimental librational energies as expected from the model of Hewson.

It is possible to compare tunnelling and structural information with ab-initio and molecular-mechanics calculations of the methyl environment.

5. Computational method

5.1. Internal barrier

We obtained the internal barrier by ab-initio calculations using the program GAMESS-UK [11,25]. These calculations are valid for the isolated molecule, the potential energy $V(\phi)$ describes the internal rotation of one part of the molecule (rotor) relative to the remainder.

We performed calculations using Hartree–Fock [26] SCF method, with the 6-31g* polarisation basis set [27]. 6-31g comprises inner shell atomic orbitals each represented by 6 Gaussians primitives. Two basis functions have been allocated to describe each valence atomic orbital. The first one is described by 3 Gaussians and the second only by one Gaussian primitive. 6-31g* is constructed by addition of 6 second-order (d-type) gaussian primitives to the 6-31g basis set description of each heavy atoms.

We generated the other conformations from the experimental geometry by rotation of the rigid methyl groups by steps of 10°.

We optimized the geometry, whilst the methyl groups were constrained to be symmetric (we used the same variable for 3 C–H lengths and the same variable for the 3 CCH angles). The principle of the geometry optimization of a molecular system is to search the atomic coordinates corresponding to the minimum energy of the system.

5.2. External and total rotational barrier

We calculated the external contributions, van der Waals (vdW) and electrostatic (Coulomb), by molecular mechanics using the commercial program Cerius² and a general pair-potential [12].

We used the crystallographic structure as a model for the following calculations. The methyl groups were symmetrized as geometric average of crystallographic data (C–H length, CCH and HCH angles).

We used a general pair-potential, universal force-field (UFF) [28], which includes almost the entire periodic table. It uses general rules for estimating force-field parameters based on simple relations. Parameters are based on the element, its hybridization and connectivity.

We calculated non-bond interaction with the Ewald summation method [29]. Non-bond interaction is calculated for pairs of atoms within a specified cutoff distance, beyond which interactions are ignored. But this direct atom-based approach becomes slow for large cutoff distances and the use of a small cutoff distance introduces errors if the interaction potential drops off slowly. The Ewald method converts non-bond terms into two sums in the real and the reciprocal space. These 2 sums are rapidly converging. Then, a cutoff distance may be applied.

In the UFF, the vdW component is given by the Lennard-Jones potential 12-6: $E_{LJ} = ar^{-12} - br^{-6}$ (a and b are constants and r is the interatomic distance). However, it has been shown that for short distances (shorter than vdW radii) the repulsive part of the potential is overestimated [30]. We used a more reasonable form of vdW interactions, given by exponential 6 potential:

$$E_{\text{vdw}}(R) = D_0 \left\{ \left[\left(\frac{6}{\gamma - 6} \right) \exp \left(\gamma \left(1 - \frac{R}{R_0} \right) \right) \right] - \left[\left(\frac{\gamma}{\gamma - 6} \right) \left(\frac{R_0}{R} \right)^6 \right] \right\} \quad (3)$$

where R is the inter-atomic distance, D_0 the bond strength, R_0 the bond length, and γ a scaling factor (typically 12).

We obtained Coulomb interactions by the charge-equilibration method (Qeq) [31] which takes into account molecular geometry, electronegativities of atoms and molecular conformation. The Qeq approach uses experimental data (atomic ionization potential, electron affinities, and atomic radii) plus electrostatic interactions between charges. The other conformations were generated from the crystallographic geometry by rigid rotation of the 2 methyl groups. We performed a charge equilibration at each step of the rotation.

Rotational and vibrational modes are not in the same energy range and coupling with vibrational

motions is considered as negligible. Further, we performed the measurements at such low temperature (ca. 2 K) that excited vibrational levels are not occupied and we can assume that during methyl rotation, the environment remains static. We will discuss intermolecular rotor-rotor coupling separately.

6. Discussion

6.1. Internal barrier: Ab-initio calculations

In the isolated molecule, the two methyl groups are equivalent. The main problem in ab-initio calculations is to choose the model. On the one hand, we can use the crystallographic structure determined at low temperature, the geometry being symmetrized by averaging the distances, angles and dihedral angles. On the other hand, we can use the optimized geometry, the methyl group being constrained to be symmetric (the 3 C-H distances, HCH and CCH angles have to be identical). It is remarkable that the methyl-group geometries are almost the same in all the models.

According to ab-initio calculations, the maximum-energy orientation for one methyl group is with a C-H bond exactly in the pyrazine ring plane and pointing towards the N-atom (noted A), this orientation is now chosen as the reference corresponding to the angular coordinate $\phi = 0^\circ$. The minimum is related by 60° rotation around the rotational axis: $\phi = 60^\circ$ (noted B). It appears clearly that the conformation BB ($\phi_5 = \phi_6 = 60^\circ$) is the minimum-energy conformation in the isolated molecule and AA is the maximum-energy conformation. In contrast, in the crystal, the experimental conformation is an AB conformation ($\phi_5 = 0$, $\phi_6 = 60^\circ$, Fig. 2).

We consider the calculated barrier of one methyl group, the other being fixed in B or A orientation (Fig. 7a and b, respectively). In both cases, the calculated internal barrier has a threefold symmetry. The magnitude of the calculated barrier depends on the model used (experimental or optimized): The main difference between the 2 models being the geometry of the pyrazine ring (Table 1). It depends also on the basis sets. The barrier of one methyl group is 13.6 meV (Fig. 7a) when the other methyl

group is fixed in B orientation, and 16.9 meV (Fig. 7b), when the other methyl group is fixed in the A orientation.

More simple basis sets are available for ab-initio calculations, for example the basis set 3-21g. The inner shell functions are written in terms of a linear combination of 3 Gaussians, the 2 valence shells are represented by 2 and 1 Gaussians, respectively. For reason of time, most applications are best carried out at 3-21g level rather than the larger 6-31g* representation. But the results for the 3-21g and the 6-31g* basis sets are comparable (see Tables 1 and 2). A

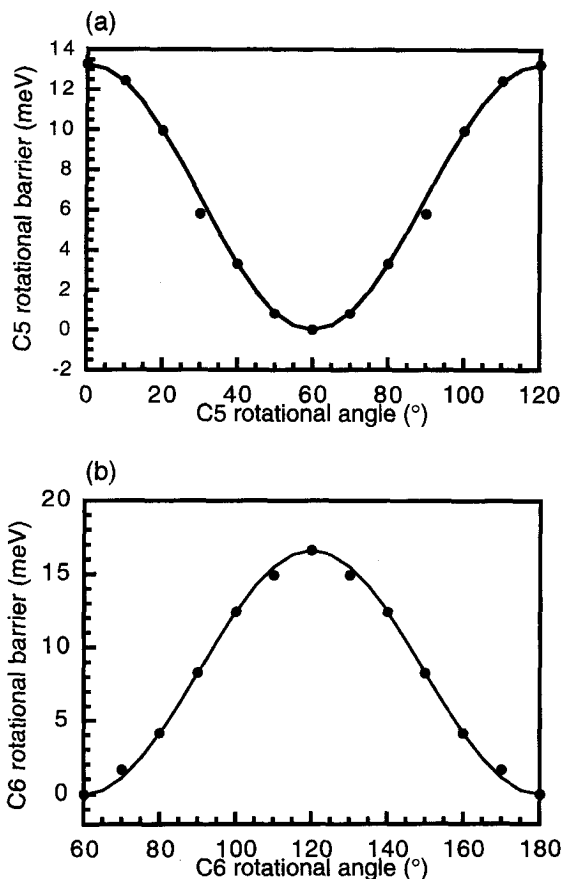


Fig. 7. Internal rotational barrier calculated by ab-initio method. The measured points were fitted with a cosine function; (a) internal barrier of C5-type, C6 being fixed in B conformation, the curve being $8.31 - 8.31 \cos(3\phi)$; (b) internal barrier of C6-type, C5 being fixed in A orientation, the curve being $6.64 + 6.64 \cos(3\phi)$.

Table 1
Rotational barrier heights

Method		Ab-initio			
Geometry		Optimized 3-21g		Experimental 3-21g	
ϕ_5	ϕ_6	Hartrees	meV	Hartrees	meV
0	0	-338.84824	0.00	-338.84567	0.0
0	60	-338.84858	9.87	-338.84602	9.52
60	60	-338.84884	16.45	-338.84631	17.4

Method		Ab-initio			
Geometry		Optimized 6-31g*		Experimental 6-31g*	
ϕ_5	ϕ_6	Hartrees	meV	Hartrees	meV
0	0	-340.76344	0	-340.76103	0.0
0	60	-340.76407	17.2	-340.76162	16.8
60	60	-340.76458	30.9	-340.7621	30.4

Method		Semi-empirical			
Geometry		Optimized AM1		Experimental AM1	
ϕ_5	ϕ_6	kcal/mol	meV	kcal/mol	meV
0	0	30.441	0.00	35.669	0.00
0	60	30.624	7.90	35.775	4.57
60	60	30.814	16.15	36.019	15.15

(a) The internal barrier heights, obtained by ab-initio method, in function of the model used: Optimized geometry or the experimental geometry described in Table 2 and in function of the rotational angle of methyl C5 and methyl C6: ϕ_5 and ϕ_6 , respectively. The angle are in degrees and the barrier heights are in meV.

(b) The total barrier heights of each methyl groups, and their 3 components: Internal, vdW and Coulomb contributions are in meV and the relative phase angle of each component, the reference being the internal component, are given in degrees.

Energies of different methyl orientations (given by the rotational angle ϕ_5 and ϕ_6 in $^\circ$) determined by different methods: (I) Total energies in Hartrees and relative energies in meV calculated by ab-initio method (the Hartree is an atomic unit of energy: 1 Hartree = 27.19 eV). (II) Heat of formation in kcal/mol and relative energies in meV calculated by semi-empirical method.

more approximate solution of the Schrödinger equation can be obtained by semi-empirical method, generally used in the analysis of large molecule to save computational time. The semi-empirical method treats only valence electrons and uses various approximations. Experimental data (like ionization potentials) are introduced in the energy expression to replace parts of the full ab-initio Hartree-Fock theory (to reduce the calculations). There are different

Table 2

Molecular geometries used for ab-initio calculations: on one hand, the optimized geometry, the methyl groups being constraint to be symmetric, and on the other hand the low-temperature structure determined from neutron diffraction, the methyl-group geometry being symmetrized by averaging distances, angles and dihedral angles (the distance are given in Å and the angles in degrees)

Geometry Basis	Optimized			Experimental
	3-21g	6-31g* AM1		
<i>Pyrazine ring</i>				
C1–C2	1.385	1.391	1.427	1.399
C1–N1	1.328	1.317	1.346	1.341
N1–C4	1.328	1.317	1.347	1.338
C4–C3	1.385	1.391	1.425	1.403
C3–N2	1.328	1.317	1.357	1.341
N2–C2	1.328	1.317	1.355	1.344
C2–C1–N1	120.5	121.2	122.3	122.5
C1–N1–C4	119.1	117.8	116.5	116.3
N1–C4–C3	120.5	121.2	122.2	122.1
C4–C3–N2	120.5	121.2	121.0	120.4
C3–N2–C2	119.1	117.8	117.1	117.5
N2–C2–C1	120.5	121.2	120.9	120.7
C1–H11	1.069	1.075	1.103	1.095
C4–H41	1.069	1.075	1.103	1.091
C2–C1–H11	119.8	119.4	121.1	120.4
C3–C4–H41	119.8	119.4	121.2	120.5
C2–C6	1.506	1.507	1.491	1.499
C3–C5	1.506	1.507	1.491	1.503
C6–C2–C1	121.6	121.2	119.8	121.5
C5–C3–C4	121.6	121.2	119.8	120.4
<i>CH₃ groups</i>				
C5 type				
C–H	1.083	1.084	1.118	1.085
COH	110.3	110.7	110.1	110.7
C6 type				
OH	1.083	1.084	1.118	1.081
COH	110.3	110.7	110.4	110.9

semi-empirical Hamiltonians. One of them, MNDO [32,33], was used in a previous work [24]. MNDO predicts that the BB conformation corresponds to a minimum-energy conformation for the isolated molecule and AA to the maximum-energy. This is in dramatic conflict with our ab-initio results. We used the more recent semi-empirical Hamiltonian AM1 [34], and we found a good agreement with the ab-initio method. Clearly, the empirical parameters used in

MNDO are not suitable for this molecule, in contrast with AM1.

Without experimental measurements of the potential (for example, in gas phase), it is difficult to choose the model. Fortunately, the difference in barriers between these models is small enough compared to external contributions that the choice between the models does not change the total barrier significantly. We continue this work with the ab-initio 6-31g* basis set and the experimental geometry of the molecule.

However, in all the calculations, the calculated barrier height of one methyl group depends weakly on the orientation of the other. This clearly means that there is a coupling between the two methyl groups (this kind of internal coupling has already been observed in other systems such as propane [27]).

A coupling between two methyl groups 5 and 6 modifies the potential-energy operator as follows [14]:

$$\begin{aligned}
 V(\phi_5, \phi_6) &= \frac{1}{2}V_3^5(1 - \cos(3\phi_5)) + \frac{1}{2}V_3^6(1 - \cos(3\phi_6)) \\
 &+ \frac{1}{2}V_6^5(1 - \cos(6\phi_5)) + \frac{1}{2}V_6^6(1 - \cos(6\phi_6)) \\
 &+ \frac{1}{4}V_3'(1 - \cos(3\phi_5))(1 - \cos(3\phi_6)) \\
 &+ \frac{1}{4}V_3''\sin(3\phi_5)\sin(3\phi_6) + \dots \quad (4)
 \end{aligned}$$

where ϕ_5 , ϕ_6 are the angles of rotation of the 2 rotors, the terms V_3^5 , V_3^6 , V_6^5 , V_6^6 are the barrier heights and the terms in V_3' and V_3'' represent the interaction of the rotors. In the isolated 2,6-dimethylpyrazine, the 2 methyl groups have the same three-fold barrier heights. If we define the effective barrier height of the methyl 6 as:

$$V_{\text{eff}}(\phi_6) = \frac{1}{2}V_3 + \frac{1}{4}V_3'(1 - \cos(3\phi_6))$$

we can easily determine the coupling term by representing this barrier as a function of ϕ_6 . Applied in the case of 2,6-dimethylpyrazine, the value of the coupling term is 3.29 meV for a barrier height of 6.58 meV. The coupling term can enhance or reduce the single particle potentials, depending of the sign of the coupling term, and the potential becomes more complex with more than 2 tunnelling lines being expected [14].

6.2. Molecular mechanics calculations

Crystallographically, the two methyl groups are inequivalent and in an antiparallel AB conformation: $\phi_5 = 0$ and $\phi_6 = 60^\circ$. Only a detailed analysis of the external components of the rotational potentials can explain the antiparallel constrained conformation, which is contrary to that found in the isolated molecule. We apply molecular mechanics calculations of these external components as described in a previous section. Considering the calculated rota-

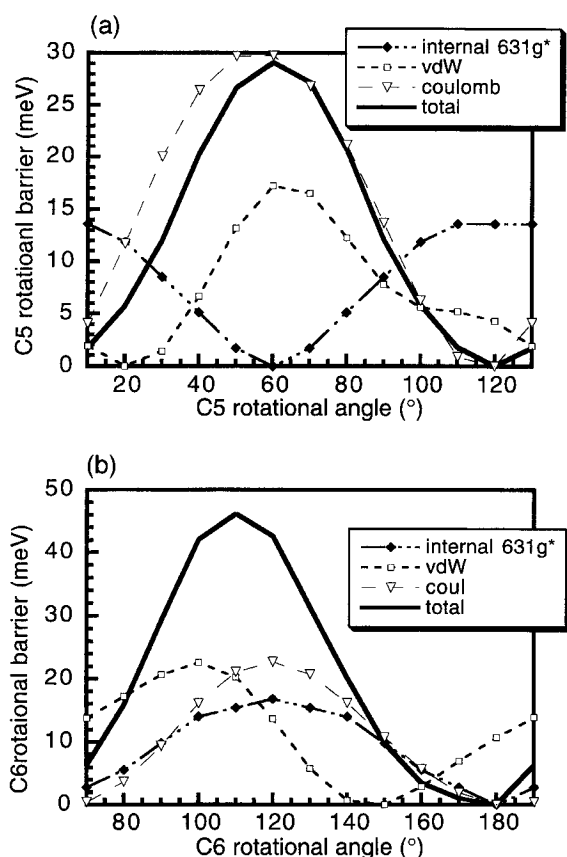


Fig. 8. Calculated rotational potentials with the internal part being calculated by ab-initio method, the external part being calculated by molecular mechanics method with a standard pair potential. The total potential is shown by a solid curve, the vdW component by the dashed curve with solid square, the Coulomb component by the dotted curve with the open square and the internal part by a dotted curve with open triangle; (a) C5-type rotational potential, C6-type being fixed in B orientation; (b) C6-type rotational potential, C5-type being fixed in A orientation.

Table 3

The rotational potentials, their internal, van der Waals (vdW) and Coulomb components and their relative phases for the C5 and the C6-types of methyl groups

	C5		C6	
	Barrier (meV)	Phase ($^\circ$)	Barrier (meV)	Phase ($^\circ$)
Total	29.1	0	46.2	0
Internal	13.6	60	16.8	10
vdW	17.2	20	22.6	-20
Coulomb	29.8	60	22.8	10

tional-potential of one methyl, the other being fixed in the experimental orientation, a reasonable agreement is found between the calculated rotational barrier 29.08 meV for C5-type (Fig. 8a), 46.16 meV for C6-type (Fig. 8b) and the measured barrier: 21.7 and 24.4 meV, respectively and the two rotational potentials are found to be pure threefold as we tentatively proposed from the experiment. If we consider that there is no coupling, we can calculate the tunnel splitting and the librational transitions of the two rotors (see Section 3). The calculated tunnel splittings are 10.9 and 1.5 μeV for the C5-type and the C6-type methyl groups, respectively, (and we observe 29 and 20 μeV), and the librational transitions are 11.2 and 14.7 meV (the observed being 8 and 10 meV respectively). The calculation is based on standard pair potential without any refinement, and we find a factor of 1.34 and 1.89 between the calculated and the observed rotational potentials for the C5-type and the C6-type, respectively. Because of the exponential dependence of the tunnel splitting there is a factor of 0.38 and 0.08 between the calculated and the observed tunnel splittings for the C5-type and the C6-type, respectively. We did not refine the potential parameters, because of the lack of observables. Vibrational spectroscopy would provide more observations, which combined with the two tunnelling lines would enable the potential parameters to be improved. Such study will be the subject of future work.

The amplitude and the phase of each contributions are collected in Table 3. The calculations show clearly that the antiparallel conformation has the lowest energy ($\phi_5 = 0$, $\phi_6 = 60^\circ$). When $\phi_6 = 60^\circ$, the main contributions to the C5-type methyl group

rotational-potential are the external interactions which are antiphase with the internal contribution (Fig. 8a). Then the A orientation becomes the minimum-energy orientation in the crystalline state for the C5-type methyl group. When $\phi_5 = 0^\circ$, the 3 contributions are almost in phase, the B orientation is still the minimum-energy orientation in the crystalline phase (Fig. 8b). Fig. 9a–c are the maps of internal, vdW and Coulomb energies, respectively, as a function of the rotational angles ϕ_5 and ϕ_6 . These figures show

clearly that the antiparallel conformation arises exclusively from external contributions.

The advantage of molecular mechanics calculations is to allow the analysis of the contributions of each atoms to the rotational potential. A detailed analysis of the different vdW contributions indicates that the most important contribution to rotational potentials is between protons of different types methyl-groups in the same plane but on different molecules. This is confirmed by a simple AM1

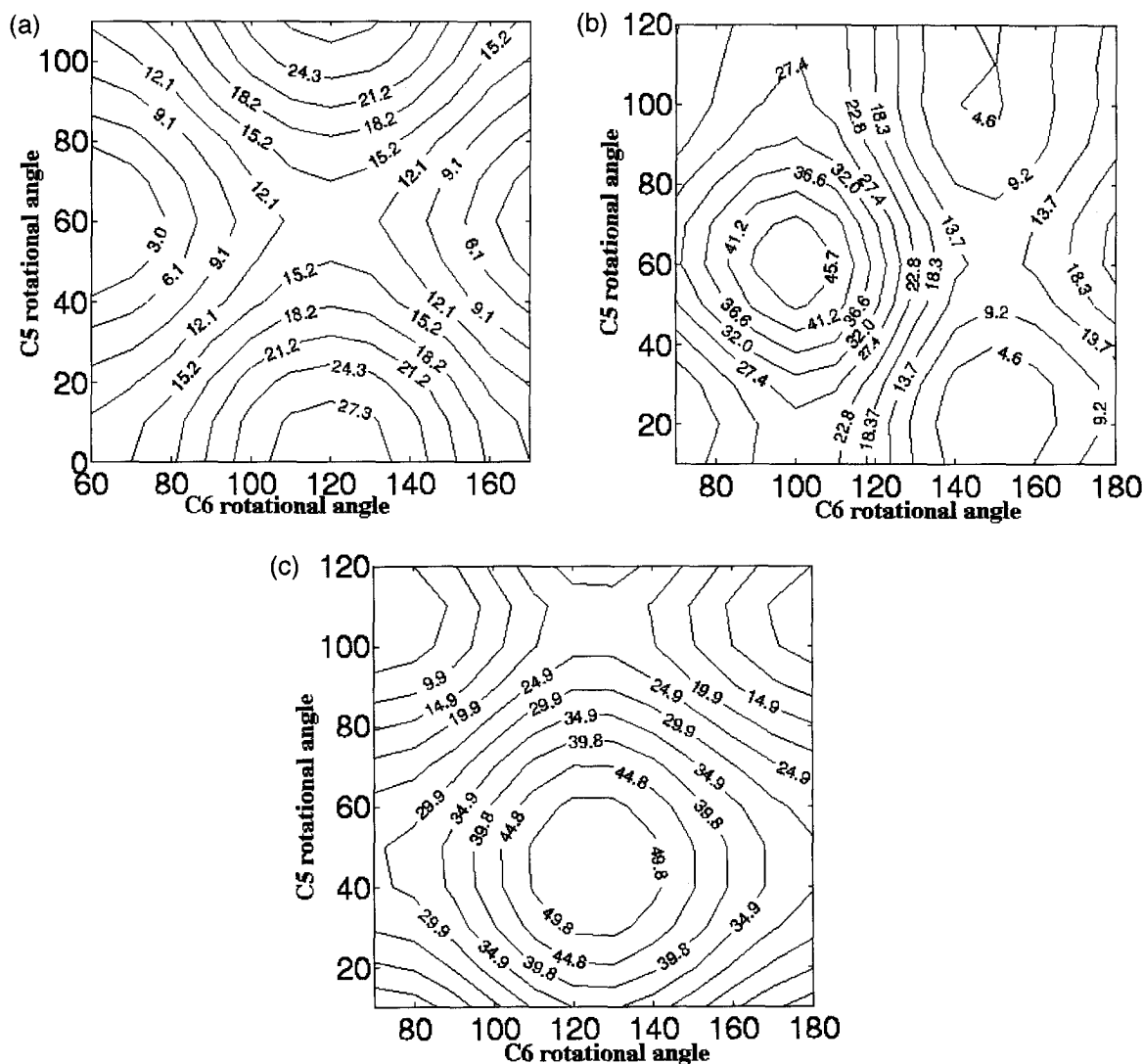


Fig. 9. Calculated contour maps of the rotational potentials as a function of the rotational angle of C5-type methyl group and C6-type methyl group; (a) internal contribution; (b) vdW contribution; (c) Coulomb contribution.

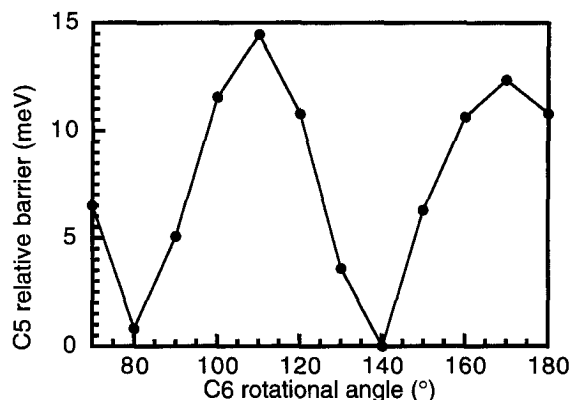


Fig. 10. Evaluation of the coupling between the 2 types of methyl groups.

semi-empirical study on a model of closest neighbouring molecules (the molecules are placed in the relative positions determined by neutron diffraction). It is obvious that such simple model cannot account to the complete rotational potential of each methyl groups but it is adequate to determine the dependence of the rotational barrier on one methyl group as a function of the orientation of the other. The barrier of one methyl group depends clearly on the orientation of another methyl group, and most of this effect arises between methyl groups of different types on different co-planar molecules (as predicted by molecular mechanics). There is an intermolecular coupling of 14.4 meV (Fig. 10). All the other coupling terms between methyl groups linked to different molecules are found smaller than 2 meV, except between 2 C5-types methyl groups lying in parallel layers: We found 8.6 meV.

7. Conclusion

INS with an oriented single-crystal allows unambiguous assignment of the tunnelling lines observed to each of the crystallographic inequivalent methyl groups. A combined use of ab-initio and molecular mechanics with the experimental structure at low temperature enables us to achieve a reasonable agreement between the observables and the calculation. The orientation of each methyl groups in the crystal as determined by neutron diffraction, the

energy range of the tunnelling frequencies, the librations, and the threefold shape of the rotational potentials are in agreement with those predicted. We determine that this molecular conformation arises exclusively from intermolecular interactions, the three contributions, internal, vdW and Coulomb being important to determine the height and the shape of the rotational potential of each methyl group. In the work presented here, only default potentials are used, and these work reasonably well. With more data these potentials could be improved.

Acknowledgements

We thank J. Goddard from the Laboratoire de Physique des Solides (Orsay, France) for providing the monocrystal sample of 2,6-dimethyl pyrazine. We are also grateful to M.R. Johnson, M. Neumann and P.H. Trommsdorff for helpful discussions and to O. Randl for help with the experimental work.

References

- [1] W. Press, Springer Tracts Modern Phys. 92 (1981) 1.
- [2] M.R. Johnson, M. Neumann, B. Nicolai, P. Smith, G.J. Kearley, *J. Chem. Phys.* 215 (1997) 345.
- [3] D. Cavagnat, A. Magerl, C. Vettier, S. Clough, *J. Phys. C* 19 (1986) 6665.
- [4] P.J. Breen, J.A. Warren, E.R. Bernstein, J.I. Seeman, *J. Am. Chem. Soc.* 109 (1987) 3453.
- [5] M. Prager, R. Hempelmann, H. Langen, W. Müller-Warmuth, *J. Phys. Condensed Matter* 2 (1990) 8625.
- [6] J. Meinel, M. Mani, M. Nusimovici, C.J. Carlile, B. Hennion, R. Carrie, B. Wynche, M. Sanquer, F. Tonnard, *Physica B* 202 (1994) 293.
- [7] J. Meinel, M. Mani, F. Tonnard, M. Nusimovici, M. Sanquer, *CR Acad. Sci. Paris* 317 (2) (1993) 885.
- [8] F. Fillaux, C.J. Carlile, *Phys. Rev. B* 42 (10) (1990) 5990.
- [9] F. Fillaux, C.J. Carlile, G.J. Kearley, M. Prager, *Physica B* 202 (1994) 302.
- [10] E. Kaiser, B. Nicolai, W. Paulus, A. Cousson, F. Fillaux, G. Heger, G.J. Kearley, O. Randl, *Acta Cryst. B* (1997) in press.
- [11] Computing for Science (CFS), Daresbury Laboratory, UK. Generalised Atomic and Molecular Electronic Structure System, 1995.
- [12] BIOSYM/Molecular Simulations, 9685 Scranton Road San Diego USA, 92121-3752. Cerius², 1996.
- [13] E. Kaiser, W. Paulus, A. Cousson, Z. Kristallograph. (1997) submitted for publication.

- [14] S. Clough, A. Heidemann, A.H. Horsewill, M.N.J. Paley, *Z. Phys. B* 55 (1984) 1.
- [15] A. Heidemann, H. Friedrich, E. Günther, W. Häusler, *Z. Phys. B Condensed Matter* 76 (1989) 335.
- [16] C.J. Carlile, S. Clough, A.J. Horsewill, A. Smith, *Chem. Phys.* 134 (1989) 437.
- [17] D. Cavagnat, J. Lacombe, J.C. Lassegues, A.J. Horsewill, J.B. Suck, A. Heidemann, *J. Physique I* (1983) 97.
- [18] G. Voll, *Physica B* 202 (1994) 239.
- [19] F. Fillaux, G.J. Kearley, C.J. Carlile, *Physica B* 226 (1996) 241.
- [20] F. Fillaux, C.J. Carlile, G.J. Kearley, *Phys. Rev. B* 44 (22) (1991) 12280.
- [21] M. Havighorst, M. Prager, *Physica B* 226 (1996) 178.
- [22] M. Neumann, G.J. Kearley, *Chem. Phys.* 215 (1997) 253.
- [23] P. Schiebel, A. Hoser, W. Prandl, G. Heger, W. Paulus, P. Schweiss, *J. Phys. Condensed Matter* 6 (1994) 10989.
- [24] J.F. Arenas, J.T. Lopez-Navarette, J.I. Marcos, J.C. Otero, *J. Mol. Struct.* 197 (1989) 87.
- [25] B. Nicolai, G.J. Kearley, O. Randl, F. Fillaux, P.H. Trommsdorff, *Physica B* 234–236 (1997) 76.
- [26] W.J. Hehre, L. Radom, P.R. Schleyer, J.A. Pople, *Ab-initio Molecular Orbital Theory*, Wiley-Interscience, New York, 1986.
- [27] L. Radom, J.A. Pople, *J. Am. Chem. Soc.* 92 (16) (1970) 4786.
- [28] A.K. Rappé, C.J. Casewitt, K.S. Colwell, W.A. Goddard Jr., W.M. Skiff, *J. Am. Chem. Soc.* 114 (1992) 10024.
- [29] N. Karasawa, W.A. Goddard, *J. Phys. Chem.* 93 (1989) 7320.
- [30] M. Prager, W.I.F. David, R.M. Ibberson, *J. Phys. Chem.* 95 (4) (1991) 2473.
- [31] A.K. Rappé, W.A. Goddard Jr., *J. Phys. Chem.* 95 (1991) 3358.
- [32] M.J.S. Dewar, W. Thiel, *J. Am. Chem. Soc.* 99 (1977) 4899.
- [33] M.J.S. Dewar, W. Thiel, *J. Am. Chem. Soc.* 99 (1977) 4907.
- [34] M.J.S. Dewar, *J. Am. Chem. Soc.* 107 (1985) 3902.